On Fair Attribution of Costs Under Peak-Based Pricing to Cloud Tenants

NEDA NASIRIANI, CHENG WANG, GEORGE KESIDIS, and BHUVAN URGAONKAR,
Pennsylvania State University
LYDIA Y. CHEN and ROBERT BIRKE, IBM Research, Zurich

3

The costs incurred by cloud providers towards operating their data centers are often determined in large part by their peak demands. The pricing schemes currently used by cloud providers to recoup these costs from their tenants, however, do not distinguish tenants based on their contributions to the cloud's overall peak demand. Using the concrete example of peak-based pricing as employed by many electric utility companies, we show that this "gap" may lead to unfair attribution of costs to the tenants. Simple enhancements of existing cloud pricing (e.g., analogous to the coincident peak pricing (CPP) used by some electric utilities) do not adequately address these shortcomings and suffer from short-term unfairness and undesirable oscillatory price-vs.-demand relationships offered to tenants. To overcome these shortcomings, we define an alternative pricing scheme to more fairly distribute a cloud's costs among its tenants. We demonstrate the efficacy of our scheme under price-sensitive tenant demand response using a combination of (i) extensive empirical evaluation with recent workloads from commercial data centers operated by IBM and (ii) analytical [modeling] through non-cooperative game theory for a special case of tenant demand model.

CCS Concepts: • **Networks** → **Cloud computing**; • **Computing methodologies** → **Modeling methodologies**; **Systems theory**; *Model verification and validation*; Computational control theory; • **Information systems** → *Data centers*; Computing platforms

Additional Key Words and Phrases: Cloud tenant, pricing design, game, fairness

ACM Reference Format:
Neda Nasiriani, Cheng Wang, George Kesidis, Bhuvan Urgaonkar, Lydia Y. Chen, and Robert Birke. 2016. On fair attribution of costs under peak-based pricing to cloud tenants. ACM Trans. Model. Perform. Eval. Comput. Syst. 2, 1, Article 3 (October 2016), 28 pages.
DOI: http://dx.doi.org/10.1145/2970815

1. INTRODUCTION

Cloud computing is turning information technology (IT) into a utility wherein cloud providers hide the complexity of building and operating data centers from their customers ("tenants") and supply them with virtualized IT resources. Inevitably, this virtualization creates a "gap" between how cloud providers incur costs for operating their data centers and how they recoup these costs from their tenants, the latter typically in terms of virtualized IT resources such as virtual machines (VMs). One important

This work was supported, in part, by the following: NSF CCF #1228717, NSF CAREER award 0953541, Swiss NSF #200021 and #141002, and EC commission under FP7 GENiC 608826.
Authors' addresses: N. Nasiriani and C. Wang, 349 IST Building, The Pennsylvania State University, University Park, PA, 16802, USA; emails: nun129@sce.psu.edu, cxw967@cse.psu.edu; G. Kesidis, 338J IST Building, The Pennsylvania State University, University Park, PA, 16802, USA; email: gik2@psu.edu; B. Urgaonkar, 338D IST Building, The Pennsylvania State University, University Park, PA, 16802, USA; email: bhuvan@cse.psu.edu; L. Y. Chen and R. Birke, BM Research Zurich, Säumerstrasse 4, CH-8803 Rüschlikon, Switzerland; emails: {yic, bir}@zurich.ibm.com.

DOI: http://dx.doi.org/10.1145/2970815

example of this gap is the difference that often exists between pricing schemes underlying costs incurred by cloud providers versus those used by cloud providers themselves to sell virtualized IT resources [Nasiriani et al. 2015].

The Problem: Several important components of a cloud provider's costs are significantly affected by the *peak* of its resource usage. Arguably, the most explicit example of this—our focus in this article—is found in the form of electric bills using "peak-based pricing" that certain electric utility companies employ, for example, see SCEG [2014] and Duke [2014]. In this pricing, the consumer's electric bill contains a separate component for its peak power draw over the billing cycle ("peak charge") *in addition to* the usual component based on energy consumed ("energy charge"). It is well known that the peak-related component can contribute a lot to the overall electric bill of the cloud provider [hamiltonblog 2014; Wang et al. 2012b]. As an example, if the peak draw is 24% more than average demand, then 50% of overall electricity bill will be due to its demand charge component.

Whereas demand response (DR) for optimizing costs under such pricing has received a lot of attention recently [Chase 2014; Wierman et al. 2014; Wang et al. 2012b], we identify a *novel* and *complementary* concern that we find useful to think of as a "fairness" problem. Notions of fair pricing of tenants in our problem are more complex than simple notions of proportional or max/min fairness due to a plurality of quantities used (mean and peak) for pricing and the complex statistics of the coincident/aggregate peak itself.

Our problem is most clearly understood by posing the following question in a revenue-neutral cloud environment: *How should a cloud provider subject to peak-based pricing for its electric power consumption recoup these costs from its tenants?* Whereas the answer is straightforward for the energy charge making up the bill (simply charge each tenant for its own total energy consumption), it becomes less clear when one considers recouping the peak charge. It is easily seen that existing pricing schemes employed by cloud providers amount to distributing the peak charge among tenants in proportion to their resource allocations (e.g., VMs) or, as a first-order approximation, in proportion to their energy consumption. We find such a pricing scheme to be "unfair" since it charges two tenants identically even if one of them contributes more to the cloud's overall peak power draw than the other (Figure 2 shows a simple example). In fact, as we show in Section 2, even other pricing schemes that do incorporate the tenants' contributions to the cloud's peak draw into their decision-making continue to suffer from such unfairness. This motivates us to explore an alternative pricing scheme that attributes peak-related costs more carefully, leading to fairer charging of tenants. We assume a revenue-neutral cloud that, by definition, ensures that the costs it recoups from its tenants are exactly what it incurs due to its own operation. However, it should be noted that our focus on a revenue-neutral cloud is a modeling choice for ease of explanation but the ideas apply to non-revenue neutral cloud providers, too. In particular, for-profit clouds may charge their tenants proportionate to their attributed operational expenditures (and possibly amortized capital expenditures).

Why Study This Problem? We find our problem worth studying for two main reasons. First, energy-related costs are already significant components of overall costs for many data centers and, correspondingly, of their tenants. It is likely that the relative contribution of energy costs will only continue to grow due to increasing trend of energy prices since the early 1990s, especially those for peak draw.

Second, one may wonder if our fairness[1] concern can be alleviated simply by replacing peak-based pricing [Duke 2014] with real-time pricing. In fact, many providers and

[1]In this work, "fairness" is used to refer to set of criteria that we claim to be desirable for our proposed pricing scheme. This set of criteria is sketched based on what we claim to be unfairness attributes of existing/possible baseline pricing approaches cf. Section 2.

consumers do find peak-based pricing more appealing due to the lower associated uncertainty compared to spot prices. Generally speaking, since spot prices can be highly dynamic, it may be desirable for certain energy consumers to hedge their electricity costs by buying from a third party an energy future whose form may be very similar to peak-based pricing or to explore a tradeoff between higher upfront costs vs. lower variability in subsequent spot prices. The choice of an electricity pricing structure for a cloud provider depends on its demand properties (predictability, flexibility, variability, etc.) as well as the variation of the spot price, compared with the hedged rate and the peak penalty. As an example, a data center whose demand is not flexible and less variable might choose a flat rate with peak power penalty; whereas another data center with highly flexible demand, might prefer real-time energy price, if the price variation is large enough for it to do arbitrage.

A Note on Generality: Although we focus only on energy-related operational expenses, there are several other data center costs that also have a peak usage-based component (although perhaps more indirectly). Internet Service Providers (ISPs) often employ tariff schemes for bandwidth, based on a high percentile that closely resemble peak charging (e.g., 95th or 99th percentile of the empirical distribution of bytes sent per measurement window over the billing cycle). In certain multi-homed settings, a cloud provider may employ a mixture of ISPs, some that charge based on raw bytes sent (like energy charge) while others based on a high percentile (similar to peak charge) [Adler et al. 2011]. Obviously, in some cases, other costs, for example, real estate can outweigh energy-related operational costs (where rents are very high, e.g., urban areas). However major data centers are located in rural areas, and, hence, energy costs are dominant. In this study, we focus on cloud providers with power costs as major contributor to their recurrent costs. Finally, many cloud providers (e.g., public clouds such as amazon-ec2 [2014]) are perhaps best modeled as being interested in profit maximization, and the fairness concerns we discuss may seem not to be directly applicable to them. However, there are many cloud computing environments where fair cost attribution may be a valid concern. Private clouds catering to departments/groups within an enterprise are an example. Moreover, with public cloud providers becoming indispensable utility providers to many large and small customers, fairness and neutrality-related mandates will likely emerge to ensure a level playing field among their tenants. An analogy with net neutrality can be drawn to show the likely rise of this issue in near future public cloud. Hence, if neutrality becomes a regulation, fairness attribution of prices will be mandated by law. This is an open problem, though, and it has started to gain attention of some researchers [Kesidis et al. 2016; Renda 2012] and also some cloud providers. For example, Interxion, a European provider defines a cloud-neutral "colo" data center as follows: *"A truly neutral data centre provider is one that is independent of the companies colocating in the data centre, does not compete with them in any way, and offers no packaged services as part of colocation. . ."* [Interxion 2016].

Contributions: For a future revenue-neutral cloud's operational costs under peak-based pricing, we define an alternative pricing scheme to more fairly distribute these costs among its tenants. Our contributions are both in terms of empirical performance evaluation methodology and theoretical results. Our proposed pricing scheme uses the first- and second-order statistics of tenant's workloads as an effective proxy for tenants' contribution to the cloud peak. This pricing is considered for cases without and with tenants' engagement in DR. Particularly, we studied the case when tenants actively engage in DR to maximize their net utility by shedding demand. We empirically evaluate both cases, using stationary and non-stationary workloads (the former synthesized from the latter) from IBM production data centers. Here is a summary of our contributions:

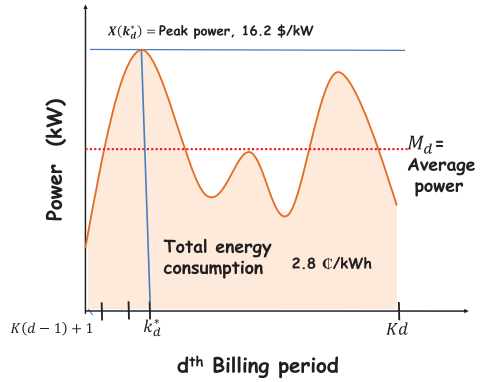

Fig. 1. An example of peak-based pricing. Tariff rates from Duke Energy.

—The performance of this pricing scheme is empirically compared against a baseline scheme through the use of recorded tenant demands from a real-world commercial data center (IBM), made challenging by the highly variable and non-stationary aspects of the workload data.
—The alternative pricing scheme under DR is studied analytically through non-cooperative game theory for a special case of tenant demand model. We show a kind of "incentive compatibility" result where tenants with higher contributions to aggregate demand variation (and hence to peak charges incurred by the cloud) pay more.

Outline: The rest of this article is organized as follows. In Section 2, we present some background and motivation using some straw-man pricing schemes. In Section 3, we define our alternative pricing scheme and carry out an empirical evaluation of its efficacy. In Section 4, we explore the impact of tenant demand-response (by demand shedding) by game-theoretic analysis and through empirical evaluation using real-world workload traces. We discuss related work in Section 5 and identify directions for future work in Section 6.

2. BACKGROUND AND MOTIVATION

We assume that our cloud provider procures electric power from an electric utility company that it uses to power its data centers (both IT equipment and non-IT infrastructure like cooling). We will use the terms "demand" and "power" interchangeably throughout the article. The cloud provider pays the electric utility company a bill at the end of dth billing period of discrete length K that has the following form:

$$P_d = \alpha K M_d + \beta X(k_d^*), \tag{1}$$

where α and β are the energy price and peak power price from the electric utility in units of \$/kWh and \$/kW, respectively. $X(k)$ denotes the cloud's power consumption during the kth time slot, $M_d = \frac{1}{K}\sum_{k=1+K(d-1)}^{Kd} X(k)$ is the mean power consumption over the dth billing period, and $k_d^* = \arg\max_k\{X(k), 1 + K(d-1) \le k \le Kd\}$ is the time slot in which the cloud's peak power demand over this billing cycle occurs. Figure 1 shows an example of such pricing. This is a simplified form of the tariff scheme employed by several electric utility companies for their large consumers. Although we choose to work with this specific pricing scheme between the utility and the data center, the problems we identify and the insights we develop likely apply more generally. For example, instead of peak-based pricing, much shorter-term (e.g., day ahead or hour

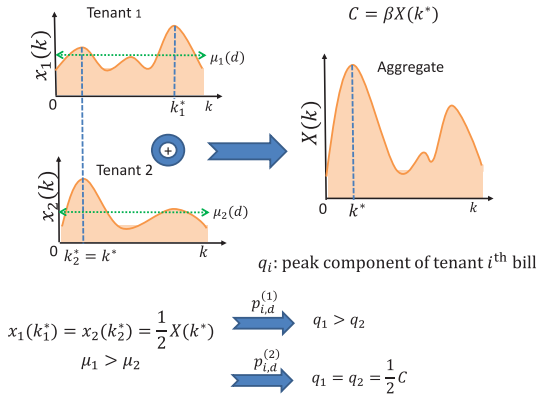

Fig. 2. Pricing based on $p_{i,d}^{(1)}$ and $p_{i,d}^{(2)}$. k^*: Cloud's peak time. k_1^*, k_2^*: Tenants' local peak time.

ahead) spot prices are often employed by electric utilities [ComEd 2014; PJM 2014]. Since such prices can be highly dynamic, it is natural for the consumer to hedge its electricity costs based on its demand properties (e.g. less variation over time) and to avoid highly uncertain spot prices. This could be through some third-party entity or directly from a power utility company that offers (presumably lower) a flat rate price and a peak penalty. The cloud provider in turn presents tenant i with a bill $p_{i,d}$ where $1 \leq i \leq N$ and all N tenants are "long-lived" in the sense of existing for the entire billing period (or several such periods).[2] We assume revenue neutrality, that is, $P_d = \sum_i p_{i,d}$. Our interest is in notions of fairness in how the provider divides P_d into $p_{i,d}$.

We make the simplifying assumption that the cloud provider has accurate power metering and accounting techniques that it can accurately partition its overall power consumption $X(k)$ during the kth time slot into $x_i(k)$, the contribution of the ith tenant. This is a complimentary problem on power metering of the VMs which uses utilization of resources such as Central Processing Unit (CPU), memory, and disk usage by the VMs [Kansal et al. 2010]. We assume the solution exists for power metering and calculating each VM contribution to the whole power consumption. We discuss three intuitively appealing "straw-man" pricing schemes and their pros and cons. Our discussion of these baseline pricing schemes helps us identify desirable features that we would like our alternative pricing scheme to possess. We propose such an alternative pricing scheme in Section 3.1.

Existing Pricing. In current cloud environments, tenants are charged based on their usage/allocation of virtualized IT resources such as VMs without distinguishing contributions to the cloud's peak demand. Our first baseline represents such pricing (hence we call it "existing pricing") and operates by dividing P_d among tenants in proportion to their mean demands over the billing cycle. That is,

$$p_{i,d}^{(1)} = \alpha K \mu_i(d) + \beta X(k_d^*) \frac{\mu_i(d)}{\sum_j \mu_j(d)}, \tag{2}$$

where $\mu_i(d)$ is tenant i's mean power demand over the dth billing period. To appreciate a key shortcoming of this scheme, consider the example shown in Figure 2, where

[2]The problem of fleeting customers is not addressed in this work. We think fleeting tenants can be considered extraneous to the fairness problem because they might not adopt contracts spanning multiple billing periods but rather prefer spot prices. These tenant will not be around for multiple billing cycles. Hence, in this work, our focus is on long-lived tenants from which accurate first- and second-order statistics are easy to calculate.

tenant 1 has higher mean demand μ and have different demand variations (and hence different contributions to the cloud's overall peak power consumption). Existing pricing results in tenant 1 being charged higher for peak contribution. However, one might find this unfair since tenant 2 contributes much more to the peak-based component of the cloud's overall costs than tenant 1.

Local-Peak Based. A second baseline scheme charges each tenant in proportion to its own "local" peak that occurs during time slot $k^*_{i,d} = \arg\max_k\{x_i(k), 1+K(d-1) \leq k \leq Kd\}$ for the ith tenant,

$$p^{(2)}_{i,d} = \alpha K\mu_i(d) + \beta X(k^*_d)\frac{x_i(k^*_{i,d})}{\sum_j x_j(k^*_{j,d})}. \tag{3}$$

This pricing scheme may seem appealing at first glance in that it allows a tenant to feel "isolated" from others.

However, such isolation holds only when all the tenants' local peaks occur together. In practice, different tenants may peak at different times, either due to inherent workload properties or due to their DR. In such cases, local peak-based pricing may be unfair to tenants that peak in a way that does not contribute to the overall peak. In Figure 2, tenants 1 and 2 have the same local peak and hence will be charged equally under this pricing; however, tenant 2 contributes much more to cloud overall peak than tenant 1. Equally problematic is that this pricing has the potential of not discouraging DR by load shifting that actually worsens the peak of the cloud's overall demand.

Contribution to Actual Peak. Alternatively, the cloud could split the peak power costs among tenants according to *their contribution* to the its overall peak. That is,

$$p^{(3)}_{i,d} = \alpha K\mu_i(d) + \beta X(k^*_d)\frac{x_i(k^*_d)}{\sum_j x_j(k^*_d)}. \tag{4}$$

This closely resembles the "coincident peak pricing" (CPP) employed by many electric utilities wherein they employ a higher-than-usual energy price during periods of high aggregate demand [coincidentPeak 2013; Liu et al. 2013]. Similarly to CPP, one simple implementation in our ecosystem could be based on the cloud sending warnings of possible coincident peaks and the tenants incorporating these warnings into their DR. One expects this pricing scheme to fairly reflect the tenant's contributions to peak power in the long term (i.e., lasting multiple billing periods). That is, in an asymptotic sense, this scheme remedies the fairness problems of the last two baselines 2. Consequently, we will use this scheme as the baseline against which we will compare our proposal in the remainder of the article.

This baseline continues to exhibit fairness problems in the short term. For a given billing period, a particular tenant may "by chance" have an unusually large $x_i(k^*)$. Such short-term unfairness may be undesirable if workload characteristics change frequently/abruptly (as we will demonstrate in Section 3.2).

3. AN ALTERNATE PRICING SCHEME

3.1. Arguments and Design

The previous discussion helps us identify two desirable features we would like to see in our alternative pricing scheme. First, it should *fairly incentivize tenant behavior that reduces overall costs*. For example, if a tenant tends to reduce its offered demand when an overall peak occurs (either inherently or via its DR), its costs should be lower than if it behaved otherwise. Second, we would like it to offer more *stable demand vs. price relation* to a tenant than the baseline does—tenants tend to prefer lower price fluctuations between billing periods as within billing periods. For example, a tenant with roughly the same demand during two different time slots should not see very different

prices, as this would complicate its decision-making. The baseline is susceptible to such behavior due to atypical events involving coincident peak occurrences only by chance.

We find two complementary design guidelines useful in achieving these desirable features.

—**Guideline A:** Our pricing scheme should fairly incorporate into a tenant's costs an explicit measure of how this tenant's demands contribute to the costs of the cloud, for example, this measure should be a reasonably accurate proxy for contribution to the cloud's peak. That is, tenant pricing should be similar to how Shapley values divide among participants the revenue gained by their coalition [Ma et al. 2008].

—**Guideline B:** A tenant's peak-related costs should be determined not merely by its contribution to the most recent billing period's peak demand (or other such potentially only "chance events") but rather by a statistical measure that can be assessed with greater confidence.

We develop our alternate pricing policy with assumptions of workload stationarity for all the tenants. Subsequently, we consider the adaptation of these basic ideas to pricing for tenants with more complex real-world workloads that are not stationary. Dropping the subscript d in the notation from Section 2 (based on our stationarity assumption), recall that over a given billing period of (discrete) time of length K, we denote as $x_i(k)$ the demand at time $k \in \{1, 2, \ldots, K\}$ of tenant i, $i \in \{1, \ldots, N\}$. Let us denote its mean as $\mu_i = \mathsf{E}x_i(k)$ and variance $\sigma_i^2 = \mathsf{E}(x_i(k) - \mu_i)^2 \; \forall k$. Let us also assume that the demands at the *same* time k of tenants i and j, $x_i(k)$ and $x_j(k)$, are correlated and define

$$c_{i,j} = \mathsf{E}((x_i(k) - \mu_i)(x_j(k) - \mu_j)).$$

As such, the cloud's aggregate demand $X := \sum_i x_i$ has mean $M = \sum_i \mu_i$ and variance $S^2 = \underline{1}^{\mathrm{T}} C \underline{1}$, where the co-variance matrix $C = [c_{i,j}]$, $\underline{1}$ is a N-vector of 1's. In this manner, our model accounts for correlated demand variation among the tenants at the same time and thus provides a simple way to explain "coincident peak" demands.

To define an alternative pricing policy, first define the $(N-1) \times (N-1)$ co-variance matrix C_{-i} without the tenant i and let $\underline{1}_{-i}$ be the $(N-1)$-vector of 1's. Also consider the aggregate demand variance without tenant i (based on guideline A above), that is, the variance of $X - x_i$,

$$S_{-i}^2 = \underline{1}_{-i}^{\mathrm{T}} C_{-i} \underline{1}_{-i}.$$

So, tenant i's contribution to the variance of the aggregate demand X is

$$S_i^2 = S^2 - S_{-i}^2.$$

Let $G(\mu, \sigma)$ be the expected peak over the billing period $\{1, 2, \ldots, K\}$ for the demand process parameterized by mean $\mu > 0$ and standard deviation $\sigma > 0$ (based on guideline B above). Our proposed pricing policy is that tenant i be charged

$$p_i^{(4)} = \alpha \mu_i K + \beta X(k^*) \frac{G(\mu_i, S_i)}{\sum_j G(\mu_j, S_j)}. \tag{5}$$

Essentially, we propose that each tenant be charged based on its mean demand and its *weighted* contribution to the cloud's peak, where the weight is a function of all tenants' expected peaks as expressed above.

Note that it is possible through negatively correlated demand that $S_i^2 < 0$, and this was observed in synthetically generated traces with negative correlation and our real-world datasets, for the latter, cf. Figures 5 and 9 in subsequent sections. In this case, a tenant may expect a discount for reducing coincident-peak power costs. So, in the

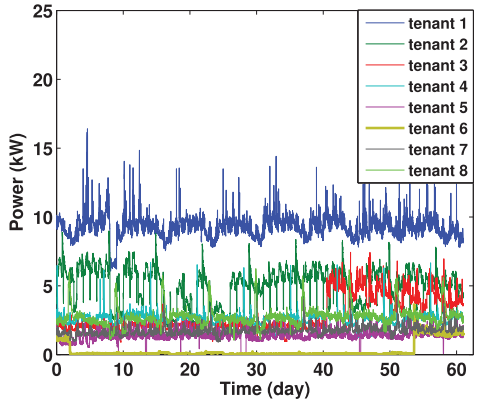

Fig. 3. Individual tenants' power demands.

above pricing formula we define

$$S_i = -\sqrt{-S_i^2} \text{ when } S_i^2 < 0. \tag{6}$$

3.2. Empirical Evaluation

In this section, we evaluate the alternative pricing design using real-world workload traces. A part of our empirical study is based on synthetic "sub-tenants" whose demands are created based on a real tenant but with special statistical behaviors to more clearly illustrate certain benefits of alternate pricing.

3.2.1. Workload Datasets. We use a set of eight tenant workload traces chosen from a production data center operated by IBM for its enterprise-scale customers. The data used for IBM real-world tenants constitute a small *portion* of the whole data-center tenants' power usage. We have chosen these eight tenants because of their special characteristics that gave us the most interesting insights. The datasets contain CPU utilization time-series for the servers allocated to these tenants. Each time-series spans 61 days and reports the average utilization over successive 15min intervals for a total of 96 samples per day. We convert these CPU utilization traces into power demands by $x_i(t) = E_{\text{PU}} n_i(t) x^{(\text{dyn})} f_i(t)$, where $n_i(t)$, $f_i(t)$, and $x^{(\text{dyn})}$ are the number of servers, average CPU utilization of tenant i at time t, and dynamic power, respectively. The power usage effectiveness (E_{PU}) of a data center is the ratio of the total power delivered to it and the power used by its IT equipment. Based on measurements from these data centers, we choose the dynamic power $x^{(\text{dyn})} = 127.7\text{W}$ and $E_{\text{PU}} = 1.8$. We ignore idle power in this study but discuss possible extensions involving it as future work in Section 6. Herein we assume power metering is possible. However, this is an open problem with certain challenges. For example, capturing shared power usage like cooling systems is hard, and ground truth is hard to measure, if at all possible. The other challenging aspect of power metering is dealing with errors, again because of absence of ground truth. These are all complexities associated with power metering, which is out of scope of this work.

We show the dynamic power consumed by each tenant in Figure 3. We take a billing period to be a single day implying 61 successive billing periods for our dataset. Although billing periods are longer in practice (e.g., a month [Duke 2014]), we choose this shorter billing period to have a large number of periods in our experiments.

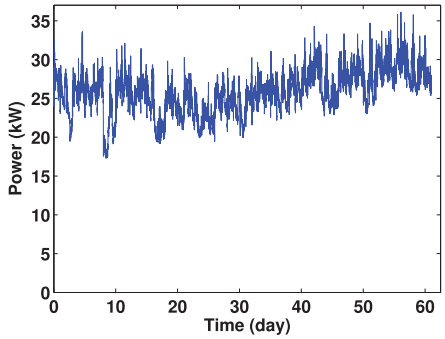

Fig. 4. Our cloud's overall power demand (summation of the tenants' demands).

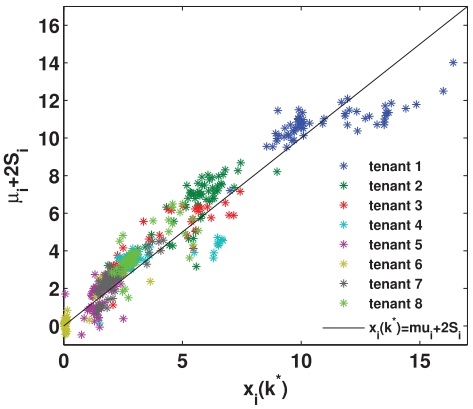

Fig. 5. $\mu_i + 2S_i$ vs. $x_i(k^*)$ from eight tenants over 61 days. Statistics are obtained on a daily basis.

We first make the following observations about individual tenants' demands: (i) some of the tenants' demands exhibit strong daily/weekly patterns, (ii) some of the tenants' demands have high fluctuations and might contribute much to the cloud's peak demand, (iii) most of the tenants' local peaks do not coincide, and (iv) some tenants' demands exhibit significant changes (e.g., tenants 3 and 6, whose demands changes abruptly after the 40th day and the 54th day, respectively). We also observe that their aggregate demand exhibits non-stationary behavior and large variations, as seen in Figure 4.

3.2.2. Experimental Setup. At the end of each day (billing period) d, each tenant i assesses its "true" mean demand $\mu_i(d)$ and demand variation $\sigma_i^2(d)$ over d, and the revenue-neutral cloud divides among the tenants its total cost as stated in (1) where $M(d)$ can be defined as $M_d = \sum_i \mu_i(d)$, $K = 96$, where $X(k) = \sum_i x_i(k)$ is the total tenant demand at time k of day d, and k_d^* is the time of the coincident (aggregate) peak demand of day d. We choose α and β according to Duke Energy tariff [Duke 2014]: $\alpha = 0.0284\$/kWh$ as energy price and $\beta = 16.193\$/kW$ as the peak power price.

To evaluate the alternative pricing, we choose $G(\mu_i, S_i) = \mu_i + 2S_i$ for our pricing formula. In spite of many possible distribution for a cloud's peak, such as Weibull or Gumbel distribution, $\mu_i + 2S_i$ is used as a proxy for tenant i's contribution to the cloud's peak for the following several reasons. First, we notice on plotting $\mu_i + 2S_i$ vs. $x_i(k^*)$ for IBM real tenants, in Figure 5, that most of the sample points are scattered closely around the line $x_i(k^*) = \mu_i + 2S_i$, where μ_i was observed to be the larger component of $\mu_i + 2S_i$. Second, we find that although the tenants' contribution to

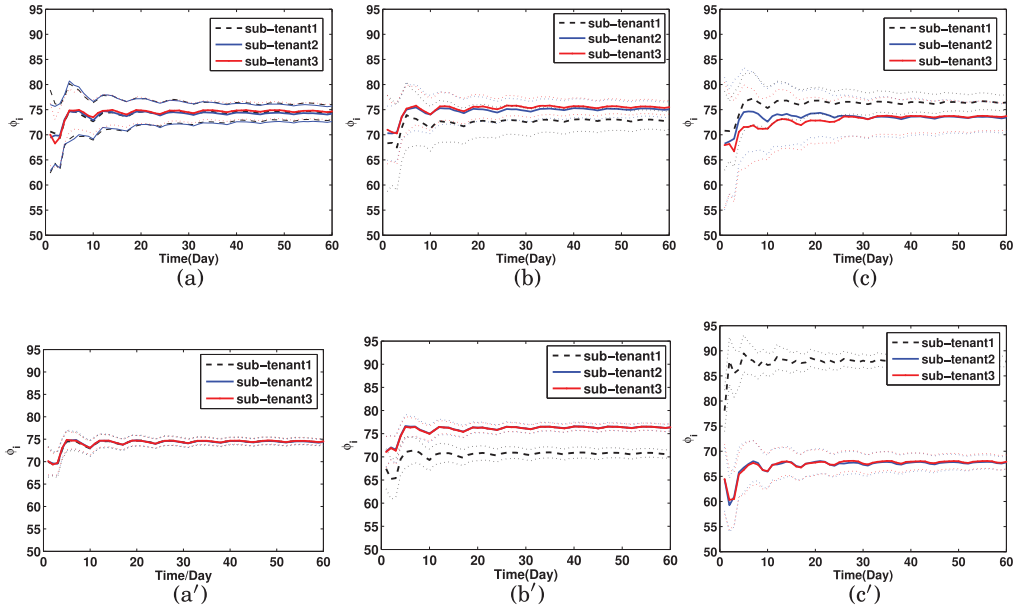

Fig. 6. Comparing baseline and alternate ($\prime$) pricing $\phi_i(d)$ without tenants' DR, 60 days, 100 sample paths, thicker lines show the average, thin-dotted lines show the width of the confidence bars ($\pm$ one sample standard deviation): (a) all sub-tenants statistically identical and uncorrelated, (b) only tenants 2 and 3 are statistically identical positively correlated, and (c) only tenants 2 and 3 statistically identical negatively correlated.

the cloud's (tenant-aggregate) peak could be high in certain billing cycles, their contribution to peak costs in the statistical sense may be relatively low (e.g., tenant 1), even negatively correlated (e.g., tenants 5 and 6). Third, we expect a tenant to have greater confidence in estimating $\mu_i + 2S_i$ than $x_i(k^*)$, which is the case, for example, for tenant 1.

3.2.3. Discussion of Performance Expectations. To evaluate the alternative pricing, we compare it with our baseline $p_i^{(3)}$. We expect the tenants' costs under alternative pricing to have lower fluctuations initially, due to estimating tenant i's contribution to the next day's peak based on the previous day's $\mu_i + 2S_i$ than by $x_i(k^*)$ (the former estimated with greater confidence). To see this, we define $\phi_i(d) = \sum_{t=1}^{d} p_i(t)/d$ as the cumulative average cost of tenant i after the dth billing cycle. We expect $\phi_i(d)$ to have lower fluctuations with alternative pricing than with the baseline CPP.

3.2.4. Cyclo-Stationary Workloads with Synthetic Sub-Tenants. In this section, we consider the demand profile of tenant 1 in Figure 3 as the aggregate demand of a hypothetical data center. This demand is modeled using estimated μ and σ of the tenant over its approximate stationary cycles, which is a week. This deterministic behavior of the tenant over time of day and time of week can be observed even visually in the same figure. Using this model, we break down the aggregate demand into synthetic demand time-series for three sub-tenants of tenant 1's real-world trace. This process is explained in detail in Appendix 7.1. We numerically compare the performance of baseline vs. alternative pricing defined in Sections 2 and 3.1.

Figure 6 depicts the cumulative average price over time for three statistical cases. The left column (case (a)) of Figure 6 is for the case of uncorrelated sub-tenants with identical workload statistics, that is, $\forall i, j$, $\mu_i = \mu_j$, and $\sigma_i = \sigma_j$. Figure 6(a) is under

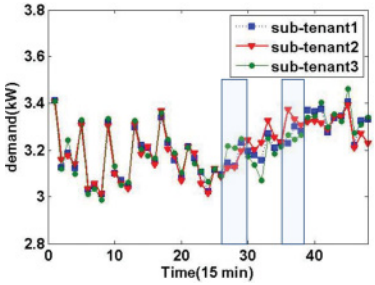

Fig. 7. One sample path for 12h (48 samples). Case (c). Two time slots with visible contribution to negative correlation are highlighted.

baseline pricing and Figure 6(a′), is under alternative pricing, as with the other two cases. For all plots: The curves of statistically identical tenants mostly overlap. It can be seen that $\phi_i(t)$ under baseline pricing has higher variation, especially in the initial billing periods. Moreover, the steady state is more quickly achieved by an alternative approach. This is consistent with the greater statistical confidence of the quantities used in alternative pricing. Again, tenants desire lower pricing fluctuations at all time-scales (including between billing periods), and baseline pricing can result in perceived "unfairness" in the short term, particularly by fleeting customers.

In case (b), sub-tenants have the same average demand, sub-tenant 1 has a higher variance than sub-tenants 2 and 3, but sub-tenants 2 and 3 are positively correlated and statistically identical such that $\sigma_1 > \sigma_2, \sigma_3$ but $S_1 < S_2, S_3$. So one expects that the positively correlated sub-tenants are charged more under alternative pricing, which is the case considering the greater gap in steady state.

In case (c), the sub-tenants have the same average demand, sub-tenants 2 and 3 are negatively correlated, sub-tenant 1 is again uncorrelated, and $\sigma_1 < \sigma_2, \sigma_3$ but $S_1 > S_2, S_3$. One sample path of this scenario can be observed in Figure 7 with time intervals contributing to negative correlation highlighted. As stated before, if two tenants are collaborating (even unintentionally) in reducing overall incident peak (through negative demand correlation), then they should be credited through a smaller peak-component cost, which is seen in Figures 6(c) and (c′): The sub-tenants with negative correlation are charged less under alternative pricing.

Key insights: (i) alternative pricing results in less variation in customers' cumulative average cost, (ii) the tenants reach their steady-state costs faster, and (iii) alternative pricing appropriately incentivize tenants behavior, including discounts for negative demand correlation.

3.2.5. Non-stationary Tenant Workloads. As in Section 3.2.4, we show $\phi_i(d)$ of each tenant under baseline vs. alternative pricing schemes over 61 days in Figure 8 here for the different recorded tenant workloads in full. For most of the tenants, we observe more fluctuations under baseline than under alternative pricing, which is consistent with our findings in Section 3.2.4. This observation is also verified by calculating the coefficient of variation over the first 20 days w.r.t. tenants' costs on the 40th day ($p_i(40)$) for each tenant,[3] which is defined as $cv_i = \frac{1}{19}\sum_{t=1}^{20}(p_i(t) - p_i(40))^2/p_i(40)$. Recall that $p_i^{(3)} = \alpha\mu_i K + \beta x_i(k^*)$ for the baseline, and we use $(\mu_i + 2S_i)$ to approximate $x_i(k^*)$. Statistically, we expect that $(\mu_i + 2S_i)$ is a good approximate and has fewer fluctuations

[3]After 40 days, tenant 3's demand changes abruptly.

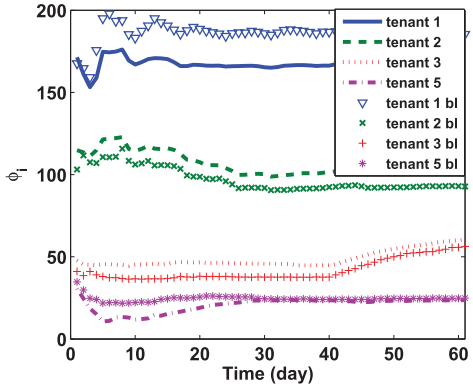

Fig. 8. $\phi_i(d)$ over 61 days (w/o tenants' DR). "bl": Baseline. See the full version in Appendix 7.3.

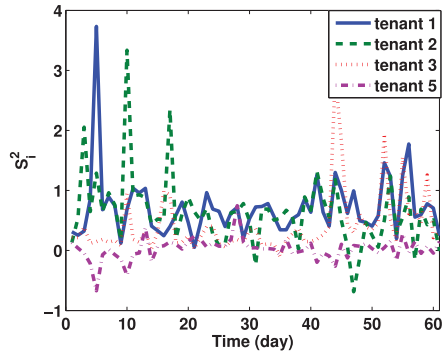

Fig. 9. S_i^2 over 61 days.

than the $x_i(k^*)$ over time, which results in less variation under the alternative than under the baseline.

We do observe one exception: Tenant 5 has more fluctuation under alternative than under baseline. This is due to the fact that S_5^2 is almost always negative for the first 15 days (as shown in Figure 9), and $x_5(k^*)$ is always positive and does not vary much (uniquely for tenant 5). Consequently, $\mu_5 - 2\sqrt{-S_5^2}$ is not as good an approximation for $x_5(k^*)$. However, consistent with the desirable properties of alternative pricing mentioned in Section 2, Tenant 5's demand is **negatively correlated** with others, which helps reduce cloud's aggregate peak demand, and samples $x_5(k^*)$ or $\mu_5 + 2\sigma_5$ do not capture such desirable negative-correlation behavior.

Figure 10 shows a comparison of some tenants' costs (tenants 1, 2, 3, and 5) for the two different pricing schemes.

We observe that tenant 1 is charged much less under the alternative than under baseline, which is because some tenants (e.g., tenant 3) might have contributed more to the cloud's peak power costs by having positive demand correlations with others, although their instantaneous share of the cloud's peak power might be relatively low. Note that tenant 5 under alternative pricing has negative costs (possibly rewards) by having negative contribution to the cloud's peak power. We also observe that after the 40th day, tenant 3's demand changes abruptly, and so does its cost. However, tenant 3's costs under alternative pricing after the 40th day has much less variation than under baseline pricing (again, this is desirable). Also, as shown in Figure 9, $S_5^2 < 0$ for the

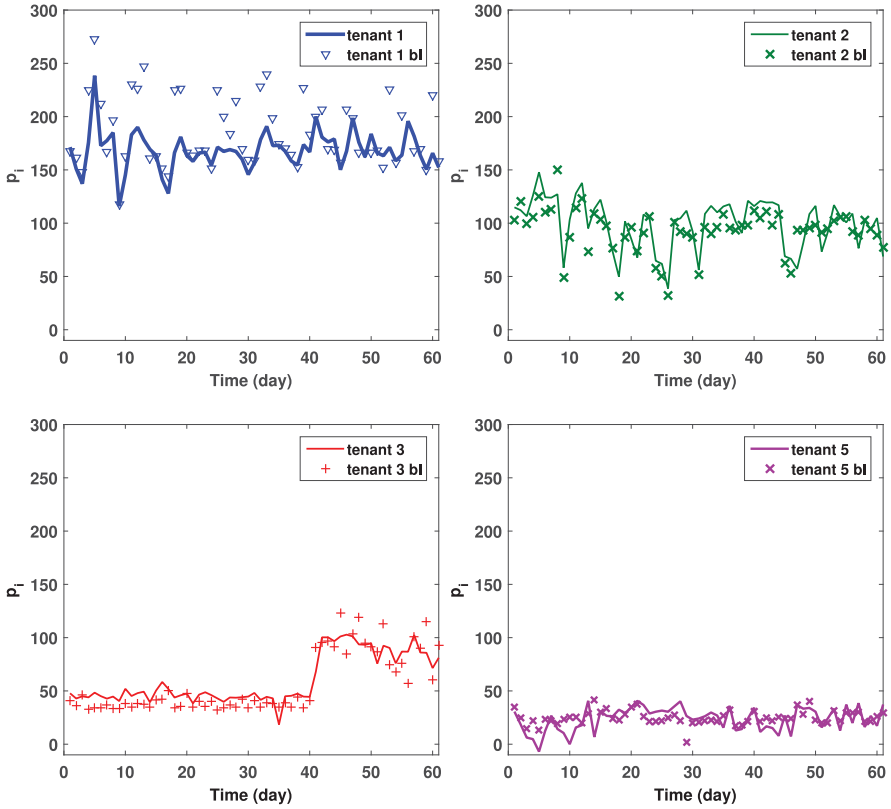

Fig. 10. Tenants' costs under baseline vs. alternative. "bl": Baseline.

first 15 days, which results in greater cost discounts for tenant 5 under alternative compared to baseline pricing, as described above.

Key insights: (i) The cumulative average costs under alternative pricing have lower variation, and (ii) alternative pricing can help the cloud motivate desirable tenant behavior by discounting tenants' with negative demand correlations.

4. COST ATTRIBUTION WHEN TENANTS ENGAGE IN DEMAND RESPONSE

We now consider the effects of tenant workload control/acutation via perfect demand shedding.[4] By supposing that each tenant handles a large and diverse job arrival process, demand shedding can be accomplished by choosing a certain proportion of incident jobs at random (in unbiased fashion) to reject, resulting in the same proportionate reduction in overall workload and power consumption of the tenant on average over a long period of time. Alternatively, a workload taxonomy can be developed and employed to classify incident jobs (and their expected workloads) and decide which ones to shed.

[4]In future work, we will consider imperfect load shedding and demand response by Dynamic Voltage and Frequency Scaling (DVFS) or load deferral as well, the latter used to desychronize tenant demands and reduce coincident peak-power consumption. Also, techniques of workload migration, leading to workload consolidation and server shutdown, have been proposed to reduce idle power in a data center [Mathew et al. 2015; Verma et al. 2010], objectives not addressed in this article.

In this section, we first prove under simplifying assumptions in an idealized setting [5] that *at Nash equilibrium*, a tenant whose demand has greater positive correlation with the aggregate other tenants will experience greater charges under the alternative pricing strategy. This simplifying assumption is made to facilitate the analysis. To study the efficacy of our proposed pricing in realistic scenarios, we relax this assumption by looking at real-world data where second-order statistics change as a result of demand shedding. Subsequently, under a more realistic setting (relaxed the simplifying assumptions) using the real-world workload traces described above, we numerically explore the effects of demand response.

4.1. A Game-Theoretic Analysis

4.1.1. Simplifying Assumptions. To develop a game-theoretic model, suppose tenant i will optimize net utility

$$v_i(\underline{\mu}) = u_i(\mu_i) - p_i(\underline{\mu}) \tag{7}$$

over their mean demand μ_i, where p_i is the "alternative" pricing scheme (5) with the aggregate peak $X(k^*)$ replaced by the "statistical aggregate peak" $M + 2S$, $\underline{\mu}$ is a vector of all tenants' mean demands, and the utility u_i is continuous, increasing, concave, and bounded. Note that Brouwer's theorem gives existence of a Nash equilibrium [Border 1985]. We make the following assumptions to simplify our analysis in this subsection:

—Observation: The tenants have perfect information regarding the statistics of their demand in the next billing cycle; in particular, the second-order statistics are used to predict contribution to coincident peak-power consumption on which the utility bases its electricity charges to the data center.[6] In the numerical experiments described in the following, second-order correlations among tenant demands were assumed estimated by the cloud based on previous demand activity; in practice, these may be noisy.
—Control: We also assume shedding load does *not* affect the second-order statistics (demand variation) of the tenants and that tenant-demand cross-correlations are non-negative.

Again, in the following numerical study, we relax these assumptions. Given the above assumption on control, we intend to prove that the Nash equilibrium prices increase with demand variation and (positive) demand correlation.

4.1.2. When Demands Are Uncorrelated. We first consider demands that are uncorrelated ($\forall i \neq j, c_{i,j} = 0$). Given this, our pricing policy in Equation (7) is taken as

$$p_i(\underline{\mu}) = \alpha \mu_i K + \beta(M + 2S)\frac{\mu_i + 2\sigma_i}{M + 2\sum_j \sigma_j},$$

where we note that

$$0 < \varepsilon := 2\left(\sum_i \sigma_i - S\right) := 2\left(\sum_i \sigma_i - \sqrt{\sum_i \sigma_i^2}\right). \tag{8}$$

[5] In particular, that demand shedding does not affect demand co-variances.
[6] Each tenant could instead formulate direct estimators of contribution to peak workload in the next billing cycle t, $\hat{x}_i(k^*(t))$, based on these quantities from past billing cycles, $x_i(k^*(s))$ for $s < t$, but the statistical confidence associated of such estimators is much lower than those for $(\mu_i + 2S_i)$ in non-stationary settings and even in stationary ones because estimates are informed by farfewer data.

The following two claims present the conditions for Nash equilibrium and the tenants' demands at Nash equilibrium.

CLAIM 1. *If C is diagonal, all utilities $u_i(\mu_i)$ are concave in μ_i, and*

$$\forall i, \sum_{j \neq i} (\mu_j + 2\sigma_j) > \mu_i + 2\sigma_i, \tag{9}$$

then there exists a unique Nash equilibrium to which "continuous best-response" (i.e., better response) dynamics,

$$\forall i, \dot{\mu}_i = \gamma_i \partial v_i / \partial \mu_i, \tag{10}$$

converge for any positive parameters $\gamma_i > 0$.

PROOF. Rosen's conditions [Rosen 1965] for uniqueness of the Nash equilibrium and convergence to it by continuous best response is that the symmetric matrix with (i, j) entry

$$\frac{\partial^2}{\partial \mu_i \partial \mu_j} (\gamma_i v_i + \gamma_j v_j)$$

is everywhere strictly negative definite. One can directly show that $\forall i, j$,

$$\frac{\partial^2 v_i}{\partial \mu_i \partial \mu_j} < 0,$$

where the claim's hypothesis implies, $\forall i \neq k$, $\partial^2 p_i / \partial \mu_i \partial \mu_k > 0$. □

Note that Equation (9) requires that the number of tenants $N > 2$. Also, Equation (9) needs to hold for all μ in a neighborhood of the unique Nash equilibrium $\underline{\mu}^*$, which we'll see from the following result is such that $\mu_i^* + 2\sigma_i = c$ for a positive constant c, that is, Equation (9) will indeed hold when $N > 2$.

Let

$$c := \frac{(N-1)\beta}{N^2(-a + \alpha K + \beta)} \varepsilon \quad \text{and}$$
$$z := \frac{\beta}{N^2} \cdot \frac{Na - \alpha K - \beta}{-a + \alpha K + \beta}.$$

The following claims how tenant charges at Nash equilibrium, p^*, (fairly) increase with tenant demand variation, σ^2.

CLAIM 2. *If C is diagonal, then*

$$\exists a > 0 \quad s.t. \quad \forall i, \quad u_i(\mu_i) = a\mu_i, \tag{11}$$

that is, linear utilities with common parameter a,

$$2 \max_i \sigma_i \leq c \tag{12}$$

and

$$\forall i, \quad (1 - \sigma_i S^{-1}) z > \alpha K, \tag{13}$$

then the prices at Nash equilibrium $\mu_i^* = c - 2\sigma_i$ satisfy

$$\forall i, \quad \frac{\partial p_i^*}{\partial \sigma_i} > 0.$$

PROOF. The solution of the first-order necessary conditions for the (unique) Nash equilibrium, $\forall i$,

$$\begin{aligned} 0 &= \frac{\partial v_i}{\partial \mu_i} \\ &= a - \alpha K - \beta + \beta\varepsilon \frac{\sum_{j\neq i}(\mu_j + 2\sigma_j)}{(\sum_j(\mu_j + 2\sigma_j))^2} \\ &=: a - \alpha K - \beta + \beta\varepsilon \frac{-\mu_i - 2\sigma_i + y}{y^2}. \end{aligned}$$

Thus, at Nash equilibrium, $\mu_i + 2\sigma_i$ is a constant over tenant-index i satisfying

$$\begin{aligned} (\mu_i + 2\sigma_i)\beta\varepsilon &=: (a - \alpha K - \beta)y^2 + \beta\varepsilon y \\ \Rightarrow y\beta\varepsilon &= N(a - \alpha K - \beta)y^2 + N\beta\varepsilon y \\ \Rightarrow y &= \frac{(N-1)\beta\varepsilon}{N(-a + \alpha K + \beta)} =: Nc. \end{aligned}$$

So, the Nash equilibrium is given by

$$\forall i, \quad \mu_i^* = c - 2\sigma_i \geq 0,$$

recalling that σ_i is assumed fixed in this section. where non-negativity is, by assumption, Equation (12). Thus, $\forall i$, the price at Nash equilibrium for tenant i, is

$$\begin{aligned} p_i^* &:= \alpha K(c - 2\sigma_i) + \beta(M + 2S)\frac{c}{Nc} \\ &:= \alpha K(c - 2\sigma_i) + \beta(Nc - \varepsilon)\frac{c}{Nc} \\ &= ((\alpha K + \beta)c\varepsilon^{-1} - \beta N^{-1})\varepsilon - 2\alpha K\sigma_i \\ &=: z\varepsilon - 2\alpha K\sigma_i \\ \Rightarrow \frac{\partial p_i^*}{\partial \sigma_i} &= z2(1 - \sigma_i S^{-1}) - 2\alpha K. \quad \square \end{aligned}$$

Note that, according to the proof, $\mu_i + 2\sigma_i = (a - \alpha K - \beta)y^2/(\beta\varepsilon) + y$ at Nash equilibrium for all tenants i, that is, each tenant's $\mu_i + 2S_i$ will be the same.

4.1.3. When Tenant Demands Are Correlated. More generally for correlated tenant demands (i.e., C is not diagonal), consider the pricing policy (5)

$$p_i(\underline{\mu}) = \alpha\mu_i K + \beta(M + 2S)\frac{\mu_i + 2S_i}{M + 2\sum_j S_j}. \tag{14}$$

In this section, we assume $S_i^2 \geq 0$ for all i (again, in the numerical section we show instances of negatively correlated tenants).

We now provide conditions for the existence of Nash equilibrium in Corollary 1 and then show that the Nash equilibrium prices increase in both their demand standard deviation σ_i as well as their demand cross-correlation $\sqrt{S_i^2 - \sigma_i^2}$ in Corollaries 2 and 3, respectively.

By the same argument for Claim 1, we get Corollary 1.

COROLLARY 1. *If all utilities u_i are concave, then*

$$\forall i, \quad \sum_{j \neq i} (\mu_j + 2S_j) > \mu_i + 2S_i$$

and

$$\sum_i S_i > S, \tag{15}$$

then there exists a unique Nash equilibrium to which "continuous best-response" (i.e., better response) dynamics,

$$\forall i, \quad \dot{\mu}_i = \gamma_i \partial v_i / \partial \mu_i, \tag{16}$$

converge for any positive parameters $\gamma_i > 0$.

LEMMA 4.1.

$$S^2 = \sum_i \sigma_i^2 + \frac{1}{2} \sum_i (S_i^2 - \sigma_i^2).$$

PROOF. Note that in $\sum_i S_{-i}^2$, the terms $c_{i,j}$, for $i \neq j$, appear $N-2$ times, while the diagonal terms $c_{i,i} = \sigma_i^2$ appear $N-1$ times. Thus,

$$\begin{aligned}
\left(\sum_i S_i\right)^2 &= \sum_i S_i^2 + 2 \sum_{j<i} S_j S_i \\
&= \sum_i (S^2 - S_{-i}^2) + 2 \sum_{j<i} S_j S_i \\
&= NS^2 - \sum_i S_{-i}^2 + 2 \sum_{j<i} S_j S_i \\
&= NS^2 - \left((N-2)S^2 + \sum_i \sigma_i^2\right) + 2 \sum_{j<i} S_j S_i \\
&= S^2 + \left(S^2 - \sum_i \sigma_i^2\right) + 2 \sum_{j<i} S_j S_i \\
&= 2S^2 - \sum_i \sigma_i^2 + 2 \sum_{j<i} S_j S_i \\
\Rightarrow S^2 &= \frac{1}{2} \left(\sum_i S_i^2 + \sum_i \sigma_i^2\right). \quad \square
\end{aligned}$$

Again, note that for the case of uncorrelated demands, $S_i = \sigma_i$ and $S^2 = \sum_i \sigma_i^2$. By Equation (17), Equation (15) holds when tenant demands are only positively correlated, that is, $\forall i, j$, $c_{i,j} \geq 0$. Because $\partial S_j^2 / \partial \sigma_j^2 = 1$, Claim 2 also generalizes by using this lemma.

COROLLARY 2. *If Equation (15), then utilities are linear with common slope $a > 0$,*

$$2 \max_i S_i \leq \quad c$$

and

$$\forall i, \quad (1 - S_i S^{-1}) z > 2\alpha K, \tag{17}$$

and then the prices at Nash-equilibrium satisfy

$$\forall i, \quad \frac{\partial p_i^*}{\partial \sigma_i} > 0.$$

COROLLARY 3. *If Equation (15), then utilities are linear with common slope* $a > 0$*,*

$$2 \max_i S_i \leq c,$$

$$\forall i, \quad \left(1 - \frac{1}{2} S_i S^{-1}\right) z > 2\alpha K, \tag{18}$$

and

$$\forall i, \quad S_i^2 > \sigma_i^2,$$

and then the prices at Nash-equilibrium satisfy

$$\forall i, \quad \frac{\partial p_i^*}{\partial \sqrt{S_i^2 - \sigma_i^2}} > 0.$$

In summary, Corollary 3 gives conditions under which the Nash equilibrium prices increase with the degree to which tenant i's demand correlates with the other tenants $\sqrt{S_i^2 - \sigma_i^2}$ to create coincident peaks in demand.

4.2. Evaluation with Tenants' Demand Response

4.2.1. Workload Forecasting Overview. In this section, we will use demand response for tenants. Causal DR will require accurate workload forecasting. Forecasting short-term (e.g., day ahead) behavior for similar such datasets has an extensive literature. For example, deterministic cyclic/seasonal components can be assessed (based on prior observations) and removed from the raw data, leaving what may be a stationary residual. Given that, one can employ standard time-invariant ARMA-type estimators [Poor 1998] whose meta-parameters (particularly lags) can also be determined by optimizing over prior observations. However, it's often unclear how much "detrending" is required (e.g., which moments) and the residual may ultimately have time-varying statistics (i.e., is non-stationary) requiring ARMA estimators with time-varying/adapted coefficients and lags. In these cases, techniques of adaptive filters such as LMS and RLS, and associated heuristics, are commonly used [Haykin 2001], often with short lags. In this article, we use first-order auto-regressive estimators, or even more simply take the previous days' data as a proxy for the next (i.e., a kind of zeroth-order estimator), and leave more sophisticated workload forecasting in this context for future work.

4.2.2. Tenants' DR under Alternative Pricing. We assume that the cloud estimates the inter-tenant demand correlations $S_i^2(d)$ over the previous day and communicates these estimates only to the corresponding tenants. At the end of day d in an alternative scenario, tenant i is charged

$$p_i^{(4)} = \alpha \mu_i K + \beta X(k_d^*) \frac{\mu_i(d) + 2S_i(d)}{\sum_j (\mu_j(d) + 2S_j(d))},$$

again recalling we set $S_i = -\sqrt{-S_i^2}$ when $S_i^2 < 0$.

For purposes of determining at the *start* of day d the fraction $1 - \lambda_i(d)$ of its demand it will shed ($\lambda_i(d)$ is the control variable), we assume tenant i will rely on a simple AR(1)

estimate of its incident demand mean,

$$\hat{\mu}_i(d) = 0.5\hat{\mu}_i(d-1) + 0.5\mu_i(d-1)/\lambda_i(d-1),^{7}$$

taking $\mu_i(0) = 0 = \hat{\mu}_i(0)$ and $\lambda_i(0) = 1$. The same model is used for estimating tenant's incident demand variation,

$$\hat{\sigma}_i^2(d) = 0.5\hat{\sigma}_i^2(d-1) + 0.5\sigma_i^2(d-1)/\lambda_i^2(d-1),$$

taking $\sigma_i(0) = 0 = \hat{\sigma}_i(0)$. We also assume that each tenant will forecast inter-tenant demand correlations for day d as that computed by the cloud for day $d-1$[8], also considering the effect of demand-shedding and assuming that other tenants will not change their shedding strategy.[9] More specifically, tenant i takes as its causal estimate of $S_i^2(d)$:

$$\hat{S}_i^2(d) = (S_i^2(d-1) - \sigma_i^2(d-1))\frac{\lambda_i(d)}{\lambda_i(d-1)} + \lambda_i^2(d)\hat{\sigma}_i^2(d).$$

Again, to determine its load shedding for day d at the *start* of day d, tenant i will optimize its net utility over $\lambda_i(d)$. Since the tenant does not have the information of $X(k_d^*)$ at the beginning of day d, it may simply take $X(k_d^*) \approx \sum_j(\mu_j(d) + 2S_j(d))$. Therefore, the net utility of tenant i can be assumed of the form

$$a_i \log\left(b_i\hat{\mu}_i(d)\lambda_i(d) + 1\right) - (\alpha K\hat{\mu}_i(d) + \beta\hat{\mu}_i(d))\lambda_i(d) - \beta 2\hat{S}_i(d).$$

4.2.3. Discussion of Performance Expectations. For our experiments, we used the same utility coefficients,[10] that is, $\forall i, j$, $a_i = a_j = a$, $b_i = b_j = b$. The correlation between tenants will still exist after DR. Therefore by the results of Section 4.1, we expect to see prices increase with tenant correlations S_i. Moreover, we expect demand shedding by tenant i will have amplified effect by reducing S_i when $S_i > 0$.

4.2.4. Cyclo-Stationary Workloads of Synthetic Sub-Tenants. In this section, we look at effects of demand response under alternative pricing for three synthetic sub-tenants. Recall from Section 3.2.4 that these sub-tenants are generated for three different cases each using time-of-day and time-of-week detrending of μ and σ derived from a real-world trace (of tenant 1 in Figure 3), as explained in Appendix 7.1.

For case (a), with uncorrelated and statistically alike tenants, the cumulative average costs (ϕ_i) and fraction of admitted demand (λ_i) under demand response for alternative pricing is given in Figure 11 (with confidence-interval outlines). The plots overlap as the tenants are statistically identical. Compared to the case without demand response in Section 3.1, steady state is reached in greater time due to the action of demand response. The sub-tenants shed on average 30% of their demand, resulting in lower prices over time. The oscillation of λ are due to a weekly pattern of raw demand used to generate the synthetic sub-tenants' demand.

For case (b), statistically identical sub-tenants 2 and 3 have positive correlation while sub-tenant 1 is uncorrelated with lower $\mu_1 + 2S_1 = \mu_1 + 2\sigma_1$. Sub-tenants 2 and 3 contribute more to aggregate demand variation ($M + 2S$) and so alternative

[7]Generally, take $\frac{0}{0} = 0$.

[8]Alternatively, the tenants could use even earlier days' estimates for this purpose.

[9]As consideration of only unilateral defection of a collective play action in the definition of a Nash equilibrium of a non-cooperative game. Indeed, were the tenant demands stationary, such daily play-actions could eventually lead to a Nash equilibrium, cf. Section 4.2.4.

[10]The effects of differences among tenant utility-parameters are straightforward, see Appendix 7.2.

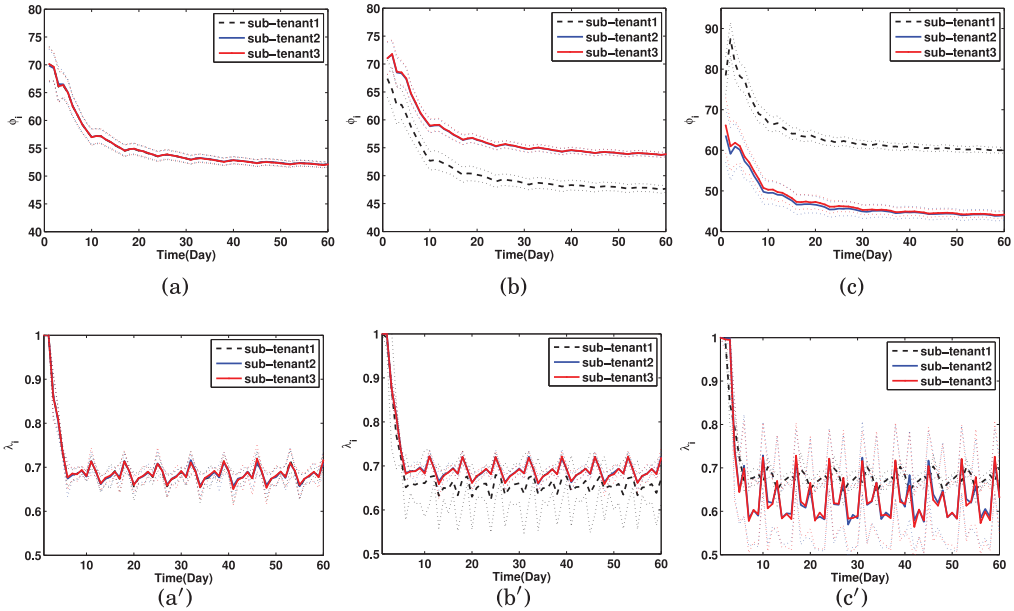

Fig. 11. $\phi_i(d)$ and $\lambda_i(d)$ $(\prime)$ after tenants' DR, 60 days, 100 sample paths; thicker lines show the average and thinner-dotted lines show the confidence bars: (a) all sub-tenants statistically identical and uncorrelated, (b) only sub-tenants 2 and 3 are statistically identical and positively correlated, and (c) only sub-tenants 2 and 3 are statistically identical and negatively correlated.

pricing charges them more than sub-tenant 1 than without demand response. However, sub-tenants 2 and 3 shed less demand than sub-tenant 1, because demand-shedding will be amplified through reducing (positive) correlation between their demands.

For case (c) in which sub-tenants 2 and 3 have negative correlation, sub-tenants 2 and 3 are charged less than without demand response. Additionally sub-tenants 2 and 3 shed *more* because demand shedding *increases* their (negative) correlation. We also observe that demand response affects S_i^2 roughly proportionate to λ_i, so the financial benefit of demand shedding in this case will depend on the relative size of mean-power and peak-power costs.

Key insights: (i) Overall S_i^2 values as main contributors to the peak-component charges are decreased considerably after demand response. (ii) Correlated tenants' shedding has a significant effect on their correlations.

4.2.5. Non-Stationary Tenant Workloads. The numerical results for the cyclo-stationary workloads of sub-tenants of tenant 1 under DR with alternative pricing are similar to those of the full (unmodified) non-stationary tenants shown in Figure 12. First note that tenant 1's control actions has less fluctuation than tenant 2, which can be explained by the fact that tenant 1's incident workload statistics $(\mu_1, \mu_1 + 2S_1)$ have less variance. Tenant 3 begins to shed load after its demand ramps up on the 40th day, whereas other tenants' demands are not shed at all. Also note that in Figure 12(b), the admitted demands of tenant 1 and tenant 2 after load shedding become more similar than their incident demands; similarly for tenant 3 after the 40th day, in part due to the assumption of the same net-utility/revenue parameters (a_i, b_i) and that the proportion of incident mean demand μ_i to S_i is roughly the same for these tenants (and this proportion does not change significantly with demand shedding). Moreover,

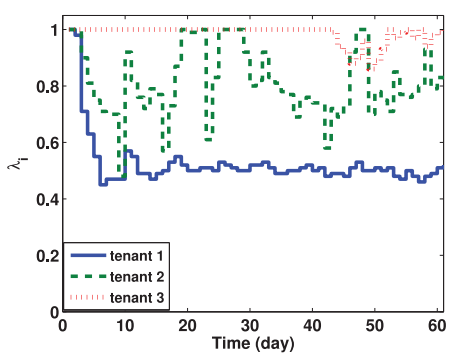

(a) Tenants' load shedding $(1 - \lambda_i)$: Ratio of raw demand that is shedded.

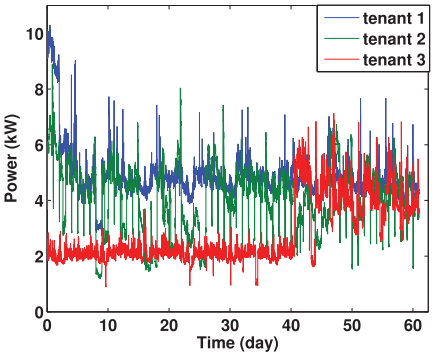

(b) Tenants' admitted demands.

Fig. 12. Non-stationary tenants' DR.

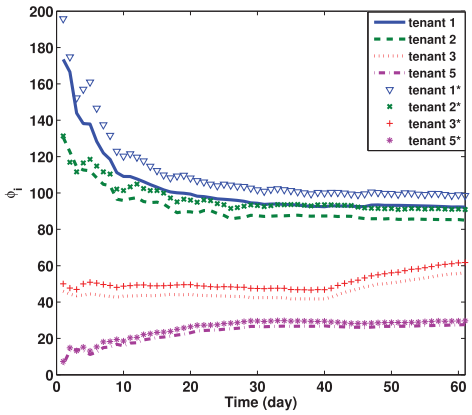

Fig. 13. Cumulative average costs with tenants DR. "*": Game with synthetic tenant 1, real tenants 2, 3, and 5.

although tenant 1 has much larger mean than tenant 2 (as shown in Figure 3), it has to shed much of its demand to maximize profit due to the log form utility function and diminishing marginal returns of increasing mean demand. Thus, these effects of DR are intuitive.

In a comparative study, we create a synthetic tenant 1 with greater demand variation as follows: We estimate the (short-term moving) average $m_1(t)$ of $x_1(t)$ (the real tenant 1's demand) and define the synthetic tenant 1's demand as $\tilde{x}_1(t) := m_1(t) + \theta(x_1(t) - m_1(t))$ for $\theta = 4$. We conduct two sets of DR experiments: one with real tenants 1, 2, 3, and 5[11] and the other with synthetic tenant 1 and real tenants 2, 3, and 5. The cumulative average costs of each tenant in both experiments are shown in Figure 13. We find that synthetic tenant 1 has much higher costs than real tenant 1 since the former's demand has much higher incident variance (and higher $c_{1,j}$ henceforth if $c_{1,j} > 0$) which does not change under DR. This is consistent with Equation (17) and Corollary 2 (obtained at Nash equilibrium in far more idealized settings). Furthermore, we observe that the other (real) tenants suffer from higher costs in the presence of synthetic tenant 1. This

[11]We choose real tenant 5 since it has little correlation or sometimes even negative correlation with tenant 1.

is because the *positive* demand cross-correlations increase when we increase tenant 1's demand variance. In other words, if a tenant is willing to reduce its demand variation (and cross-correlation) by DR, other tenants whose demands are positively correlated can benefit from it and have lower costs.

We observe that, compared to Figure 5, $\mu_i + 2S_i$ is more aligned with $x_i(k^*)$ after tenants' DR (as shown in Figure 15 in Appendix 7.3). Tenants who have larger $\mu_i + 2S_i$ before DR (e.g., tenant 1 in Figure 5) shed more demands than others, which is also consistent with our observations from Figure 12(b).

Key insights with DR: (i) Tenants' load shedding exhibits lower fluctuation when the workloads have less variance. (ii) Tenants are likely to have the same/similar mean demand (but with different variance possibly) when they have the same parameters for utility functions. (iii) Even with load shedding, tenants with higher variance will have higher costs. (iv) Tenants with positively correlated demands can benefit from each other's load shedding.

5. RELATED WORK

Pricing design in clouds. The first line of related work on cloud pricing design is driven by energy costs. In particular, a large body of work has explored dynamic pricing under time-varying electricity prices. In Zhan et al. [2015], a game-theoretic setting is proposed, considering cloud green generation, to maximize revenue and incentivize tenants' cooperation in response to the electricity charges reflected in cloud prices. In another recent work [Zhao et al. 2014], dynamic pricing for a geo-distributed data center is suggested to maximize cloud's overall profit (being charged by spot prices for power) using an online algorithm. In Ren and Mihaela [2014], dynamic pricing and scheduling for batch jobs are proposed for cloud's profit maximization based on Lyapunov optimization technique. In Wang et al. [2015], a leader/follower game-based cloud pricing framework is devised to recoup dynamic energy costs from tenants. However, our focus on the impact of electric utility tariff structure (especially the impact of peak-based pricing) on the cloud's pricing strategies (and the tenants' DR in terms of power thereafter) is novel. Recent work has also looked at cloud's DR and related pricing design given that electric utility might motivate load shedding/peak shaving during high load periods in the form of rewards. In Ren and Islam [2014] and Zhang et al. [2015b] a reverse-auction framework is proposed for co-location data centers to incentive tenant's DR for cloud's profit optimization with utility's rewards. Similarly, in Liu et al. [2014], a prediction-based pricing scheme is proposed to encourage tenant's load shedding in order to meet a certain peak shaving target specified by the electric utility. The key distinguishing aspect of our work is its focus on notions of fairness. The pricing schemes developed in all these works are likely to suffer from the unfairness problems and oscillatory costs for tenants that we identified for our baseline. Our work distinguishes by considering peak-based pricing as a less risky approach for cloud providers' electric bills and also considering fairness and stability of the costs incurred to the tenants.

A second line of prior work focuses on pricing of general computing resources/serivces in the cloud such as VM, network bandwidth, storage, software service, and so on. Various techniques such as dynamic pricing [Kantere et al. 2011], auction-based pricing [Shi et al. 2014; Zhang et al. 2015a; Wang et al. 2012a; Baranwal and Vidyarthi 2015; Zhang et al. 2015a; Shi et al. 2014], Nash bargaining [Feng et al. 2012] with either single or multiple strategic cloud providers [Feng et al. 2014; Anselmi et al. 2014], and game theory [Tsai and Qi 2012] considering Cournot duopoly, Cartel and Stackelberg models. In Valerio et al. [2013], a two-stage provisioning scheme is used wherein the second stage uses a Stackelberg setup to determine number of flat-rate, on-demand, and

spot-priced VMs to be procured from infrastructure as a service (IaaS). Moreover, different dynamic pricing approaches have been proposed by researchers, considering different objectives and methods, for example, targeting a power usage capacity [Polverini et al. 2013] using an online algorithm, maximizing profit using an stochastic dynamic programming [Xu and Li 2013], and maximizing social welfare while providing stochastic guarantees of network bandwidth for cloud tenants [Niu et al. 2012]. These works only look at the computing resource supply-vs.-demand relationship between cloud and tenants, whereas our work focuses on cloud's peak-based energy costs; it is non-trivial to attribute such costs together with computing resources/services to the tenants in a fair manner, and our method of identifying tenant's contribution to cloud's peak power costs is novel in this area.

Data-center power management. Data-center power management (including DR) has been explored extensively, and we only cite a few representative examples. We find it useful to classify DR-related work along two dimensions. First, a variety of power/resource control techniques have been explored. One may view these as being (often implicitly) based on demand shedding (e.g., admission control, equipment slow/shutdown, quality-of-service reduction) [Gandhi et al. 2009; Mathew et al. 2015; Gandhi et al. 2012; Xu and Li 2014], demand delaying (e.g., scheduling) [Zhu et al. 2014; Ge et al. 2012], demand transfer (e.g., migration) [Qureshi et al. 2009], demand modulation using batteries [Wang et al. 2012b; Urgaonkar et al. 2011], or combinations of these. Second, DR algorithms have been developed for a variety of pricing schemes, including coincident peak pricing [Liu et al. 2013], peak-based pricing [Bar-Noy et al. 2008], and many forms of real-time pricing [Wang et al. 2014]. Although we have only considered a simplified form of load shedding as our DR, we take other control knobs as possible extensions to our work. Finally, two detailed surveys cover many of these issues and serve as excellent resources for understanding this area [Chase 2014; Wierman et al. 2014].

6. DIRECTIONS FOR FUTURE WORK

In future work, we will attempt to extend our analytical results to consider effects on second-order statistics of demand shedding and to consider noisy observations and play-actions (the latter informed by more sophisticated workload forecasting for the next billing cycle). Also, using our real-world datasets, we will consider other types of demand response, for example, DVFS or demand deferral via scheduling, possibly in combination with demand shedding. Moreover, we will explore the performance benefits of techniques of workload migration, leading to workload consolidation and server shut-down, which have been proposed to reduce idle power in a data center. Finally, we are pursuing more detailed workload classification that indicates workload of specific arriving jobs; with such data, we may be able to to formulate a job taxonomy and classification system to predict sensitivity to deferral[12] and the demand footprint of specific jobs and thus improve the accuracy of workload shedding in particular.

7. APPENDIX

7.1. Generating Synthetic Component Tenants

In this appendix, we describe how the sub-tenants demands are generated. First, let $x(t)$ be the raw demand of tenant 1 of Figure 3. The time interval of the trace was approximately 8 weeks (with a sample every 15min), so there are 8 samples taken at the same time of the same day of week. For each sample t during this 8-week period, let

[12]Excessive job deferral may amount to dropping.

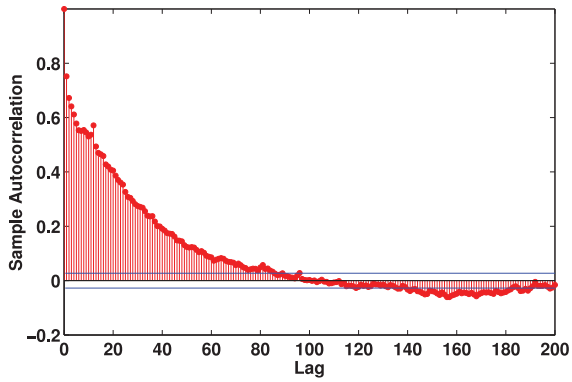

Fig. 14. Autocorrelation of detrended tenant demand.

$\delta(t)$ be the day of the week and $\tau(t)$ be the time of day. A pattern was observed for these data over each week, which can be easily observed in Figure 3. Therefore, we removed this pattern by removing the periodic time-of-day and time-of-week effect $\bar{x}(\delta(t), \tau(t))$ from the raw trace $x(t)$. The obtained residual after detrending is as follows:

$$r(t) = x(\delta(t), \tau(t)) - \bar{x}(\delta(t), \tau(t)),$$

where

$$\bar{x}(\delta(t), \tau(t)) = \frac{1}{8} \sum_{\substack{s:\delta(s)=\delta(t) \\ \text{and } \tau(s)=\tau(t)}} x(s).$$

In Figure 14, we show the autocorrelation function of (mean zero) residual r, which is approximately white as we subsequently assume for simplicity.[13] Given this assumption, we can compute the sample variance of the residual r at each time-of-day,

$$\sigma^2(\delta(t), \tau(t)) = \frac{1}{8} \sum_{\substack{s:\delta(s)=\delta(t) \\ \text{and } \tau(s)=\tau(t)}} r(s)^2.$$

By using this model which is based on first- and second-order statistics of the raw data, we can model synthetic sub-tenant data. Therefore, $\bar{x}(\delta(t), \tau(t))$ and $\sigma^2(\delta(t), \tau(t))$ are broken down to desired number of tenants by fixed weight matrices $\mathbf{A}$ and $\mathbf{D}$, respectively, over the whole period of simulation. The synthetic sub-tenant mean weight $\mathbf{A}$ and covariance matrix weight $\mathbf{D}$ is normalized so their entries $\sum_j a_j = 1$ and $\sum_{i,j} d_{ij} = 1$. This is to achieve synthetic sub-tenants data such that their aggregate behavior is statistically similar to the raw data. It is necessary that $\sum_j a_j = 1$ holds to have the same aggregate mean, and for $\mathbf{D}$, considering $var(X + Y) = var(X) + cov(X, Y) + cov(Y, X) + var(Y)$, it is desired that aggregate demand of the synthetic sub-tenant data have the same variance as the raw tenant data, which is satisfied by $\sum_{i,j} d_{ij} = 1$. Consequently, for sample t, we took the covariance of the sub-tenants to be $\sigma^2(\delta(t), \tau(t))\mathbf{D}$. So to generate the tth samples $y_j(t)$ of the jth sub-tenant, we generated i.i.d. Gaussian N(0,1) samples $w_j(t)$ and set

$$\underline{y}(t) = \bar{x}(\delta(t), \tau(t))\mathbf{A} + \sigma(\delta(t), \tau(t))\mathbf{B}\underline{w}(t),$$

[13]A more complex representation of r could be based on an FIR approximation of its inverse whitening filter (driven by actual white noise) [Poor 1998].

where **B** is a lower triangular matrix of the Cholesky decomposition of **D**. **B** is used to apply correlation between synthetic sub-tenant data to present specific cases for our study.

7.2. Discussion of Experimental Variations

There are possible variations for the set of experiments done in previous sections of this work. Some measurement and actuation errors could be introduced into the system. The source of this error could be noisy measurement or calculation of statistics of tenants as well as noise engaged in actuation for demand response.

The other variation is using different utility functions. In this study, we are using the same coefficients for utility function a and b. Therefore, tenants are shedding similarly. By adopting different a and b, sub-tenants can control the amount of their shedding. It is obvious that increasing a and b values will increase the utility and therefore decrease the amount of shedding.

7.3. Additional Figures

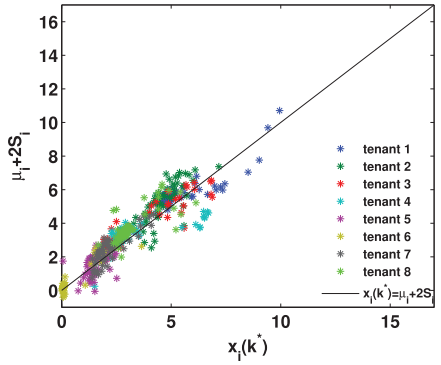

Fig. 15. $\mu_i + 2S_i$ vs. $x_i(k^*)$ with tenants' demand response.

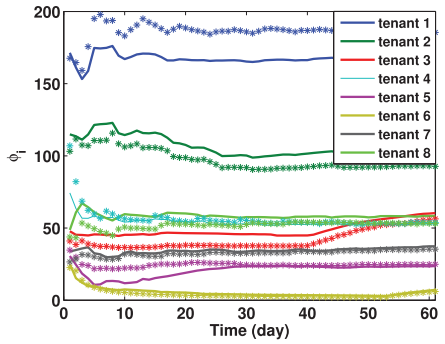

Fig. 16. $\phi_i(d) = \frac{\sum_{t=1}^{d} p_i(t)}{d}$ without tenants' demand response (61 days). The solid curves are obtained under alternative pricing while the curves with "*" represent the baseline pricing.

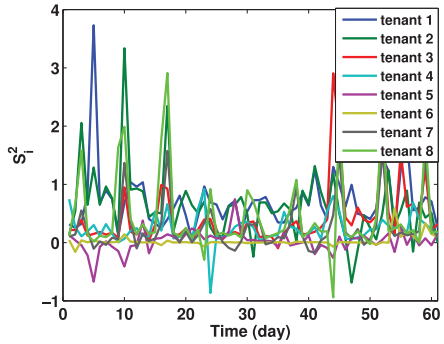

Fig. 17. S_i^2 for each tenant over 2 months without tenants' demand response.

ACKNOWLEDGMENTS

We thank the anonymous reviewers for their useful comments.

REFERENCES

M. Adler, R. K. Sitaraman, and H. Venkataramani. 2011. Algorithms for optimizing the bandwidth cost of content delivery. *Comput. Netw.* 55, 18 (2011), 4007–4020.

amazon-ec2. 2014. Amazon EC2 Pricing. Retrieved from http://aws.amazon.com/ec2/pricing/#on-demand.

J. Anselmi, D. Ardagna, J. C. S. Liu, A. Wierman, Y. Xu, and Z. Yang. 2014. The economics of the cloud: Price competition and congestion. *SIGMETRICS Perform. Eval. Rev.* 41, 4 (Apr. 2014).

A. Bar-Noy, Y. Feng, M. Johnson, and O. Liu. 2008. When to reap and when to sow: Lowering peak usage with realistic batteries. In *Proceedings of WEA*.

G. Baranwal and D. P. Vidyarthi. 2015. A fair multi-attribute combinatorial double auction model for resource allocation in cloud computing. *J. Syst. Softw.* 108 (2015), 60–76.

K. C. Border. 1985. *Fixed Point Theorems with Applications to Economics and Game Theory*. Cambridge University Press, London.

J. S. Chase. 2014. *Demand Response for Computing Centers*. Taylor & Francis.

coincidentPeak. 2013. Fort Collins Coincident Peak. Retreived from http://www.fcgov.com/utilities/business/rates/electric/coincident-peak.

ComEd. 2014. Real-time hourly prices, ComEd. Retrieved from https://rrtp.comed.com/live-prices/.

Duke Duke. 2014. Duke utility bill tariff. Retrieved from http://www.considerthecarolinas.com/pdfs/scscheduleopt.pdf.

Y. Feng, B. Li, and B. Li. 2012. Bargaining towards maximized resource utilization in video streaming datacenters. In *INFOCOM*.

Y. Feng, B. Li, and B. Li. 2014. Price competition in an oligopoly market with multiple IaaS cloud providers. *IEEE Trans. Comput.* 63, 1 (2014).

A. Gandhi, M. Harchol-Balter, R. Das, and C. Lefurgy. 2009. Optimal power allocation in server farms. In *Proceedings of ACM SIGMETRICS*.

A Gandhi, M. Harchol-Balter, and M. A. Kozuch. 2012. Are sleep states effective in data centers? In *Proceedings of IGCC*.

Y. Ge, Y. Zhang, Q. Qiu, and Y. Lu. 2012. A game theoretic resource allocation for overall energy minimization in mobile cloud computing system. In *Proceedings of the 2012 ACM/IEEE International Symposium on Low Power Electronics and Design (ISLPED'12)*. ACM, New York, NY.

hamiltonblog. 2014. James Hamilton's Blog. (2014). http://perspectives.mvdirona.com/.

S. Haykin. 2001. *Adaptive Filter Theory*. Prentice Hall.

Interxion. Retrieved from http://www.interxion.com/.

A. Kansal, F. Zhao, J. Liu, N. Kothari, and A. A. Bhattacharya. 2010. Virtual machine power metering and provisioning. In *Proceedings of SoCC*.

V. Kantere, D. Dash, G. Francois, S. Kyriakopoulou, and A. Ailamaki. 2011. Optimal service pricing for a cloud cache. *IEEE Trans. Knowl. Data Eng.* 23 (Sept 2011), 1345–1358.

G. Kesidis, B. Urgaonkar, N. Nasiriani, and C. Wang. 2016. Neutrality in future public clouds: Implications and challenges. In *Proceedings of Eurosys HotCloud 2016*.

Z. Liu, I. Liu, S. Low, and A. Wierman. 2014. Pricing data center demand response. In *Proceedings of ACM SIGMETRICS*. New York, NY.

Z. Liu, A. Wierman, Y. Chen, and B. Razon. 2013. Data center demand response: Avoiding the coincident peak via workload shifting and local generation. In *Proceedings of ACM SIGMETRICS*.

R. T. B. Ma, D.-M. Chiu, J. C. S. Lui, V. Misra, and D. Rubenstein. 2008. Interconnecting eyeballs to content: A shapley value perspective on ISP peering and settlement. In *Proceedings of NetEcon*.

V. Mathew, R. K. Sitaraman, and P. Shenoy. 2015. Energy-efficient content delivery networks using cluster shutdown. *Sustainable Computing: Informatics and Systems* 6 (2015), 58–68.

N. Nasiriani, C. Wang, G. Kesidis, B. Urgaonkar, L. Chen, and R. Birke. 2015. On fair attribution of costs under peak-based pricing to cloud tenants. In *Proceedings of IEEE MASCOTS*.

D. Niu, C. Feng, and B. Li. 2012. Pricing cloud bandwidth reservations under demand uncertainty. In *Proceedings of ACM SIGMETRICS*.

PJM. 2014. Day-Ahead Energy Market, PJM. Retrieved from http://www.pjm.com/markets-and-operations/energy/day-ahead.aspx.

M. Polverini, S. Ren, and A. Cianfrani. 2013. Capacity provisioning and pricing for cloud computing with energy capping. In *Proceedings of the IEEE Annual Allerton Conference*.

H. V. Poor. 1998. *An Introduction to Signal Detection and Estimation*. Springer.

A. Qureshi, R. Weber, H. Balakrishnan, J. V. Guttag, and B. M. Maggs. 2009. Cutting the electric bill for internet-scale systems. In *Proceedings of ACM SIGCOMM*.

S. Ren and M. A. Islam. 2014. Colocation demand response: Why do I turn off my servers? In *Proceedings of ICAC*.

S. Ren and V. D. S. Mihaela. 2014. Dynamic scheduling and pricing in wireless cloud computing. *IEEE Trans. Mob. Comput.* 13, 10 (Oct 2014), 2283–2292.

Andrea Renda. 2012. Competition, neutrality and diversity in the cloud. *Commun. Strateg.* 85 (2012), 23–44.

J. B. Rosen. 1965. Existence and uniqueness of equilibrium points for concave *N*-person games. *Econometrica* 33, 3 (1965), 520–534.

SCEG. 2014. SCE&G. Retrieved from https://www.sceg.com/docs/librariesprovider5/electric-gas-rates/rate23.pdf.

W. Shi, L. Zhang, C. Wu, Z. Li, and F. C. M. Lau. 2014. An online auction framework for dynamic resource provisioning in cloud computing. In *Proceedings of ACM SIGMETRICS*.

W. Tsai and G. Qi. 2012. DICB: Dynamic intelliegnt customizable benign pricing strategy for cloud computing. In *Proceedings of IEEE ICCC*.

R. Urgaonkar, B. Urgaonkar, M. J. Neely, and A. Sivasubramaniam. 2011. Optimal power cost management using stored energy in data centers. In *Proceedings of ACM SIGMETRICS*.

V. D. Valerio, V. Cardellini, and F. L. Presti. 2013. Optimal oriving and service provisioning strategies in cloud systems: A stackelberg game approach. In *Proceedings of ACM ICCC*.

A. Verma, R. Koller, L. Useche, and R. Rangaswami. 2010. SRCMap: Energy proportional ptorage using dynamic consolidation. In *Proceedings of FAST*.

C. Wang, N. Nasiriani, G. Kesidis, B. Urgaonkar, Q. Wang, L. Y. Chen, A. Gupta, and R. Birke. 2015. Recouping energy costs from cloud tenants: Tenant demand response aware pricing design. In *Proceedings of the 2015 ACM 6th International Conference on Future Energy Systems (e-Energy'15)*. ACM, New York, NY, 141–150. DOI: http://dx.doi.org/10.1145/2768510.2768541

Cheng Wang, Bhuvan Urgaonkar, Qian Wang, and George Kesidis. 2014. A hierarchical demand response framework for data center power cost optimization under real-world electricity pricing. In *Proceedings of IEEE MASCOTS*.

D. Wang, C. Ren, A. Sivasubramaniam, B. Urgaonkar, and H. K. Fathy. 2012b. Energy storage in datacenters: What, where and how much? In *Proceedings of ACM SIGMETRICS*.

Q. Wang, K. Ren, and X. Meng. 2012a. When cloud meets eBay: Towards effective pricing for cloud computing. In *Proceedings of the 2012 IEEE INFOCOM*. 936–944.

A. Wierman, Z. Liu, I. Liu, and H. Mohsenian-Rad. 2014. Opportunities and challenges for data center demand response. In *Proceedings of IEEE IGCC*.

H. Xu and B. Li. 2013. Dynamic cloud pricing for revenue maximization. *IEEE Trans. Cloud Comput.* 1, 2 (2013), 158–171.

H. Xu and B. Li. 2014. Reducing electricity demand charge for data centers with partial execution. In *Proc. of e-Energy*.

Y. Zhan, M. Ghamkhari, D. Xu, and H. Mohsenian-Rad. 2015. Propagating electricity bill onto cloud tenants: Using a novel pricing mechanism. In *Proceedings of IEEE Globecom*.

L. Zhang, Z. Li, C. Wu, and S. Ren. 2015b. Online electricity cost saving algorithms for co-location data centers. In *Proceedings of the 2015 ACM SIGMETRICS International Conference on Measurement and Modeling of Computer Systems (SIGMETRICS'15)*. 463–464.

X. Zhang, Z. Huang, C. Wu, Z. Li, and F. C. M. Lau. 2015a. Online auctions in IaaS clouds: Welfare and profit maximization with server costs. In *Proceedings of the 2015 ACM SIGMETRICS International Conference on Measurement and Modeling of Computer Systems (SIGMETRICS'15)*. 3–15.

J. Zhao, H. Li, C. Wu, Z. Li, Z. Zhang, and F. C. M. Lau. 2014. Dynamic pricing and profit maximization for the cloud with geo-distributed data centers. In *Proceedings of IEEE INFOCOM*.

X. Zhu, L. T. Yang, H. Chen, J. Wang, S. Yin, and X. Liu. 2014. Real-time tasks oriented energy-aware scheduling in virtualized clouds. *IEEE Trans. Cloud Comput.* 2, 2 (April 2014), 168–180.

Received October 2015; revised June 2016; accepted July 2016